AMERICAN SOCIETY FOR MICROBIOLOGY | Journal of Bacteriology®

RESEARCH ARTICLE

The *Coxiella burnetii* QpH1 Plasmid Is a Virulence Factor for Colonizing Bone Marrow-Derived Murine Macrophages

Shengdong Luo,[a,b] Shanshan Lu,[a] Huahao Fan,[a] Zeliang Chen,[a] Zhihui Sun,[b] Yan Hu,[c] Ruisheng Li,[c] Xiaoping An,[a] Vladimir N. Uversky,[d,e] Yigang Tong,[a] Lihua Song[a,b]

[a]Beijing Advanced Innovation Center for Soft Matter Science and Engineering, College of Life Science and Technology, Beijing University of Chemical Technology, Beijing, China

[b]State Key Laboratory of Pathogen and Biosecurity, Beijing Institute of Microbiology and Epidemiology, Beijing, China

[c]Research Center for Clinical Medicine, The Fifth Medical Center of PLA General Hospital, Beijing, China

[d]Department of Molecular Medicine, USF Health Byrd Alzheimer's Research Institute, Morsani College of Medicine, University of South Florida, Tampa, Florida, USA

[e]Laboratory of New Methods in Biology, Institute for Biological Instrumentation of the Russian Academy of Sciences, Federal Research Center Pushchino Scientific Center for Biological Research of the Russian Academy of Sciences, Pushchino, Moscow, Russia

Shengdong Luo, Shanshan Lu, Huahao Fan, and Zeliang Chen contributed equally to this work. Author order was determined by mutual agreement among first authors.

ABSTRACT *Coxiella burnetii* strains carry one of four large, conserved, autonomously replicating plasmids (QpH1, QpRS, QpDV, or QpDG) or a QpRS-like chromosomally integrated sequence of unknown function. Here, we report the characterization of the QpH1 plasmid of *C. burnetii* Nine Mile phase II by making QpH1-deficient strains. A shuttle vector pQGK containing the CBUA0036 to CBUA0039a region (predicted as being required for QpH1 maintenance) was constructed. The pQGK vector can be stably transformed into Nine Mile II and maintained at a similar low copy number like QpH1. Importantly, transformation with pQGK cured the endogenous QpH1 due to plasmid incompatibility. Compared to a Nine Mile II transformant of an RSF1010-ori-based vector, the pQGK transformant shows a similar growth curve in both axenic media and Buffalo green monkey kidney cells, a variable growth defect in macrophage-like THP-1 cells depending on the origin of inoculum, and dramatically reduced ability to colonize wild-type bone marrow-derived murine macrophages. Furthermore, we found that CBUA0037 to CBUA0039 open reading frames (ORFs) are essential for plasmid maintenance, and CBUA0037 and CBUA0038 ORFs account for plasmid compatibility. In addition, plasmid-deficient *C. burnetii* can be isolated by using CBUA0037 or CBUA0038 deletion vectors. Furthermore, QpH1-deficient *C. burnetii* strains caused a lesser extent of splenomegaly in SCID mice, but, intriguingly, they had significant growth in SCID mouse-sourced macrophages. Taken together, our data suggest that QpH1 encodes a factor(s) essential for colonizing murine, not human, macrophages. This study suggests a critical role of QpH1 for *C. burnetii* persistence in rodents and expands the toolkit for genetic studies in *C. burnetii*.

IMPORTANCE All *C. burnetii* isolates carry one of four large, conserved, autonomously replicating plasmids or a plasmid-like chromosomally integrated sequence. The plasmid is a candidate virulence factor of unknown function. Here, we describe the construction of novel shuttle vectors that allow making plasmid-deficient *C. burnetii* mutants. With this plasmid-curing approach, we characterized the role of the QpH1 plasmid in *in vitro* and *in vivo C. burnetii* infection models. We found that the plasmid plays a critical role for *C. burnetii* growth in murine macrophages. Our work suggests an essential role of the QpH1 plasmid for the acquisition of colonizing capability in rodents by *C. burnetii*. This study represents a major step toward unravelling the mystery of the *C. burnetii* cryptic plasmids.

Citation Luo S, Lu S, Fan H, Chen Z, Sun Z, Hu Y, Li R, An X, Uversky VN, Tong Y, Song L. 2021. The *Coxiella burnetii* QpH1 plasmid Is a virulence factor for colonizing bone marrow-derived murine macrophages. J Bacteriol 203:e00588-20. https://doi.org/10.1128/JB.00588-20.

Editor Laurie E. Comstock, Brigham and Women's Hospital/Harvard Medical School

Address correspondence to Yigang Tong, tong.yigang@gmail.com, or Lihua Song, songlihua@gmail.com.

Received 21 October 2020
Accepted 2 February 2021
Accepted manuscript posted online 8 February 2021
Published 8 April 2021

KEYWORDS *Coxiella burnetii*, intracellular pathogen, microbial pathogenesis, plasmid genetics, plasmid pathogenesis

Coxiella burnetii is a Gram-negative intracellular bacterium that causes Q fever, a zoonosis that is widely distributed in the world (1). It is highly infectious and is classified as a potential biowarfare agent (2). Its infections in humans are mostly asymptomatic but may manifest as an acute disease (mainly as a self-limiting febrile illness, pneumonia, or hepatitis) or as a chronic disease (mainly as endocarditis in patients with previous valvulopathy) (1). All *C. burnetii* isolates maintain a large cryptic plasmid or plasmid-like chromosomally integrated sequence (3). This absolute conservation of plasmid sequences suggests that they are critical in *C. burnetii* survival (4). Increased knowledge of the plasmid sequences will enhance our understanding of *C. burnetii* biology and pathogenesis and will be important for guiding the design of vaccine strains for the prevention of Q fever.

C. burnetii has at least five different plasmid types as follows: four plasmids (QpH1, QpRS, QpDV, and QpDG) and one type of QpRS-like chromosomally integrated sequence (5–9). The plasmids range from 32 to 54 kb in size and share a 25-kb core region (3). Characterization of these plasmid types led to the classification of five associated genomic groups. The hypothesized correlation of plasmid types and genomic groups with the clinical outcomes of Q fever was controversial (3, 10, 11), but the concept of genomic group-specific virulence was supported by mouse and guinea pig infection studies (12, 13). According to studies on *C. burnetii* mostly from Europe and North America, this bacterium is considered to have a clonal population structure with low genetic diversity (14–16). Future studies on more *C. burnetii* isolates, especially from other regions, will help in our understanding of its global genetic diversity.

The sequences of all five representative plasmid types in *C. burnetii* have been determined (3, 7, 8, 17, 18). Beare et al. analyzed the diversity of plasmid genes using DNA microarrays (3). Nine predicted functional plasmid open reading frames (ORFs) are conserved in all plasmid sequences. Two of these ORFs appear to encode proteins similar to phage proteins involved in tail assembly and site-specific recombination, while seven of them encode hypothetical proteins. Three (CBUA0006, CBUA0013, and CBUA0023) of these conserved plasmid hypothetical proteins are secreted effectors of the type IV secretion system (4). During ectopic expression in HeLa cells, these effectors localize at different subcellular sites, suggesting roles in subversion of host cell functions (4). In addition, novel plasmid-specific effectors were also identified, supporting the concept of pathotype virulence (19). Beside the identification of plasmid-encoded secretion effectors, the plasmid is also speculated to be able to be transferred to the host cell (20).

The advent and foregoing improvement of axenic culture techniques greatly facilitates studies on *C. burnetii* biology (21–24). *C. burnetii* replicates within phagolysosome-like parasitophorous vacuoles (termed *Coxiella*-containing vacuole [CCV]) in mononuclear phagocytes. Genetic studies revealed that the CCV biogenesis and *C. burnetii* growth in host cells require a type IV secretion system and a repertoire of type IV effectors (25–28). The role that these effectors play in *C. burnetii* pathogenicity is of intense interest. However, regarding the plasmid effectors, reports on their mutants are scarce. By using transposon mutagenesis, Martinez et al. identified mutants of eight QpH1 genes and observed strong phenotypes with mutants of *parB* and *repA*, surprisingly, not the mutant of the conserved secretion effector CBUA0023 (29). Regardless of the identification of plasmid secretion effectors, a role for the plasmid in *C. burnetii* pathogenesis remains elusive.

Since the first development of axenic media, the *C. burnetii* genetics toolbox has been expanding (30, 31). Current genetic tools for *C. burnetii* include, but are not limited to, transposon systems (32), RSF1010-ori-based shuttle vectors (4, 33), and targeted gene inactivation systems (31). However, there have been no reports of studies using these tools to decipher the roles of plasmids in *C. burnetii* pathogenesis. Here,

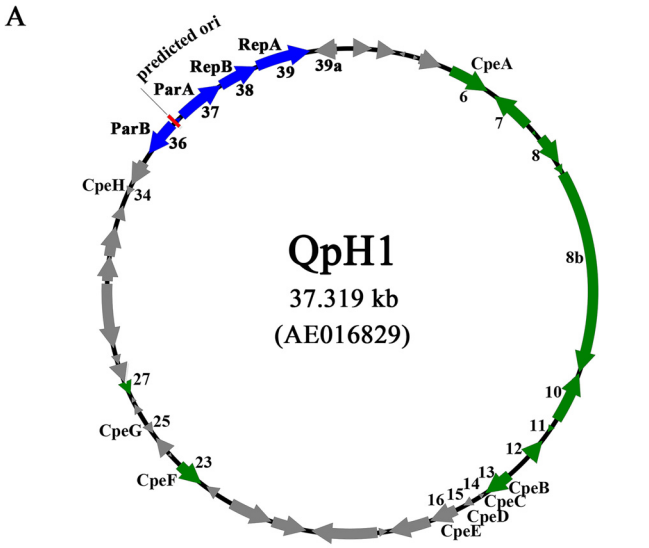

B

start	sequence	end
32514	ATACCGCAAACGTCTCGCTTT	32534
32535	..C.T.....T...G.ATA.C	32555
32556	.AC..........G.TTCC.	32576
32577	..C.T..T..T.....TTAAA	32597

FIG 1 Map of the QpH1 plasmid (A) and the sequence of its predicted origin of replication, which is composed of four 21-bp iteron-like sequences (B). (A) The conserved ORFs (green) (3), predicted ORFs for plasmid maintenance (blue), and predicted ori (red) are as indicated. (B) In the iteron alignment, dots represent nucleotides that are identical to those in the most upper iteron. The first and last nucleotides in each iteron are given as its position in the complete plasmid.

we describe a set of QpH1-derived shuttle vectors for *C. burnetii* transformation. These shuttle vectors have different compatibilities with QpH1 and different stabilities in *C. burnetii*. A QpH1-deficient strain of *C. burnetii* was constructed by transforming with the pQGK vector. Infection experiments show that QpH1 is essential for colonizing bone marrow-derived murine macrophages. This work increases our knowledge on plasmid biology and provides new genetic tools for investigating *C. burnetii* pathogenesis.

RESULTS

***C. burnetii* plasmid has a putative iteron-like origin of replication.** The QpH1 plasmid of the Nine Mile isolate is 37,319 bp in size and encodes 40 ORFs, of which only 11 are similar to proteins of known function (Fig. 1A) (18). Besides its cryptic role in pathogenesis, the plasmid's mechanism of replication and partitioning also lacks understanding. A gene cluster CBUA0036 to CBUA0039 encodes homologs of ParB, ParA, RepB, and RepA, respectively, which were previously reported as plasmid replication-associated proteins and are expected to function in plasmid replication and partitioning based on similarities with known proteins (34–38). The plasmid was found to have a low copy number (10), but its origin of replication has never been identified. With equicktandem of the EMBOSS software suite (39, 40), we found a putative origin of replication—a region composed of four 21-bp iteron-like sequences between CBUA0036 and CBUA0037 (Fig. 1B). Unlike the highly conserved iterons in other plasmids, all four iteron-like sequences in QpH1 have base variations from each other. Importantly, this putative iteron region is highly conserved in currently known *C. burnetii* plasmids. The finding of this putative iteron region suggests that genes required for QpH1 replication and partitioning are clustered.

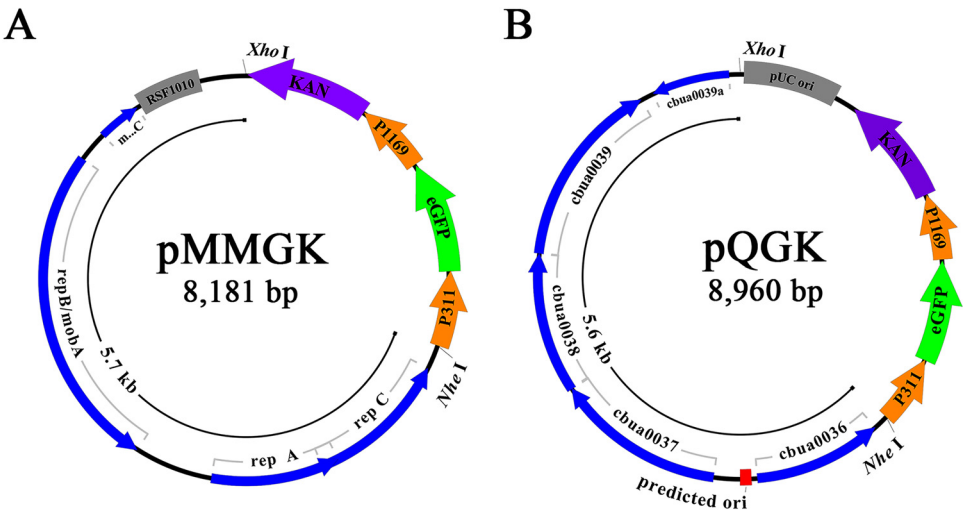

FIG 2 Map of two shuttle vectors, pMMGK (A) and pQGK (B). Both vectors share identical Kan^r and eGFP genes, driven by P1169 and P311 promoters, respectively. (A) The inner circle of the pMMGK vector represents the backbone of an RSF1010-ori-based plasmid pMMB207. (B) The inner circle of the pQGK vector represents the fragment from QpH1. The genes and their direction of transcription are represented by the boxes of the outer circle.

Construction of incompatible plasmid pQGK and curing of endogenous QpH1 from Nine Mile II by transformation. The RSF1010-ori-based shuttle vectors are routinely used for the *C. burnetii* transformation (31, 33). We first made an RSF1010-ori-based shuttle vector pMMGK for transformation (Fig. 2A). An incompatible plasmid pQGK (i.e., a plasmid, introduction of which negatively affected the inheritance of the QpH1 plasmid) was then constructed based on the clustering of genes (CBUA0036 to CBUA0039) needed for the QpH1 maintenance (Fig. 2B). The hypothetical CBUA0039a gene was also incorporated into pQGK, as this gene is located close to the CBUA0039 and might play unknown roles in plasmid maintenance. The plasmids—pMMGK and pQGK—were transformed into the Nine Mile II (NMII), thereby generating NMII*pMMGK* and NMII*pQGK* transformants, respectively. After passaging in the presence of kanamycin six to seven times, the transformants were cloned using semisolid ACCM-2 plates and characterized by PCR detection of the QpH1 ORFs. All QpH1 ORFs can be detected in NMII*pMMGK*, but only the CBUA0036 to CBUA0039a ORFs can be detected in NMII*pQGK* (Fig. 3). The absence of CBUA001 to CBUA0034a in NMII*pQGK* indicates that the endogenous QpH1 was cured by transformation of pQGK.

QpH1-deficient *C. burnetii* has normal growth kinetics in axenic media and BGMK cells. The transformants of pMMGK and pQGK—NMII*pMMGK* and NMII*pQGK*—were derived from the same Nine Mile II clone. In addition to carrying different shuttle vectors, their major genetic difference is the presence or absence of the endogenous QpH1 plasmid. Both shuttle vectors carry the enhanced green fluorescent protein (eGFP) cassette, and their clonal homogeneity can be clearly inspected by observing eGFP expression. We investigated the potential impact of QpH1 on bacterial growth with these two eGFP-labeled transformants. Their growth kinetics in ACCM-2 medium and Buffalo green monkey kidney (BGMK) cells were assessed by measuring their one-step growth curves (Fig. 4). In axenic media, these two transformants display growth kinetics similar to that of the wild-type Nine Mile II. In BGMK cell experiments, two origins of inoculum of the transformants were tested in order to evaluate the effect of the axenic media on small-cell variant (SCV) viability. We found that the two transformants also consistently showed similar growth profiles in BGMK cells. Because the NMII*pMMGK* strain has NMII-like growth profiles and can be readily observed by green fluorescent protein (GFP) expression, we frequently used NMII*pMMGK* as the sole QpH1-bearing control strain. Altogether, the two transformants displayed similar growth kinetics, suggesting that QpH1 is not important for the *C. burnetii* growth in the axenic media and BGMK cells.

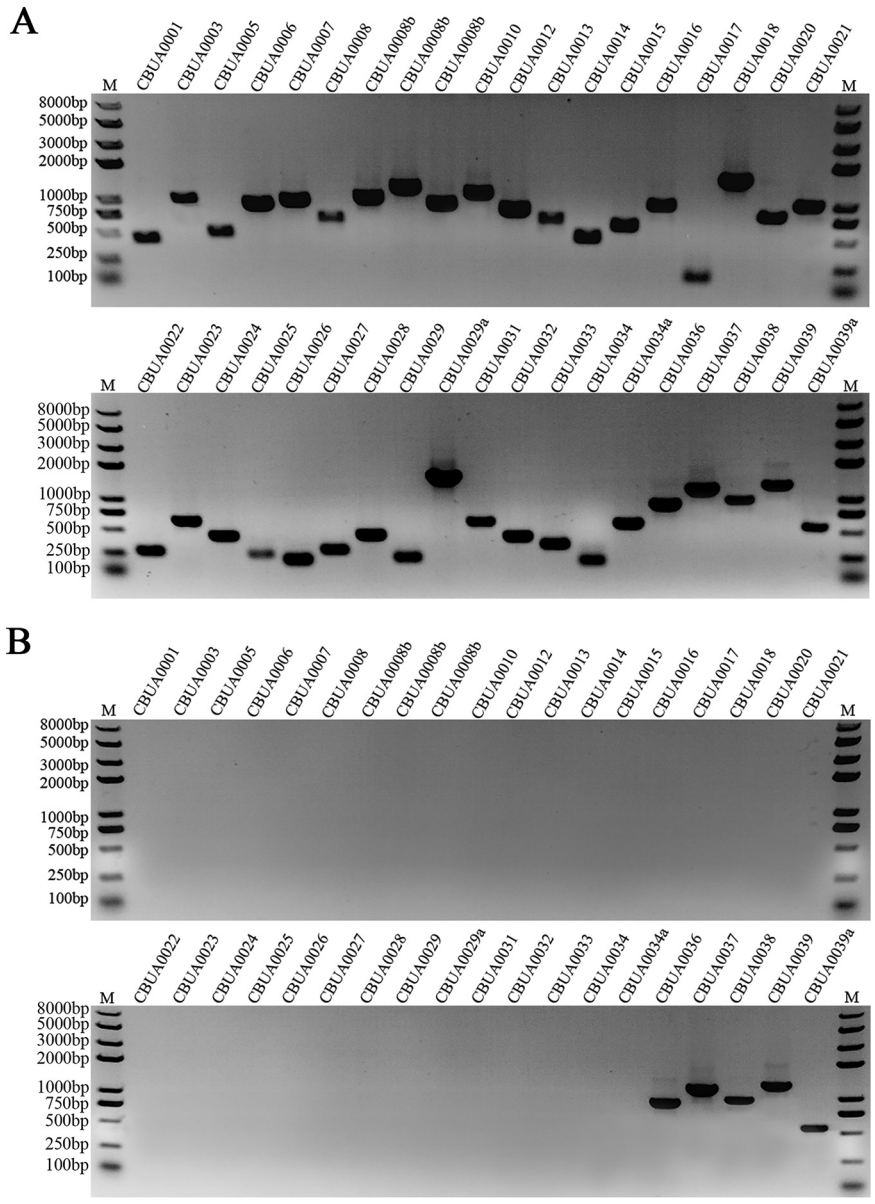

FIG 3 PCR detection of QpH1 ORFs in two transformants, NMII*pMMGK* (A) and NMII*pQGK* (B). QpH1 has about 40 ORFs. Thirty-eight primer pairs listed in Table S4 in the supplemental material were designed for PCR detection. All QpH1 ORFs are present in NMII*pMMGK* while only the CBUA0036 to CBUA0039a ORFs can be detected in NMII*pQGK*, which shows that NMII*pMMGK* is QpH1 bearing while NMII*pQGK* is QpH1 deficient.

Interestingly, though having similar growth kinetics, these two transformants differed significantly in the expression of their eGFP genes (Fig. 5). Although the eGFP genes of these two transformants had identical promoters, the fluorescence intensity of the NMII*pMMGK* appeared to be higher than that of the NMII*pQGK*. The difference in the levels of eGFP expression between these two transformants may reflect the difference in the gene copy numbers. Based on previous reports, the copy number of the RSF1010-ori-based shuttle vector is 3 to 6 (30), while the QpH1 copy number is between 1 and 3 (10). Our data show that QpH1 and pQGK have a similar copy number of about 1 (Fig. 5F), suggesting that pQGK retains all genes for QpH1 replication and partitioning. The copy number of pMMGK is about two to three times the copy number of pQGK, which is consistent with their expression levels of eGFP. Overall, our data suggest the copy number of QpH1 and pQGK is under highly stringent control.

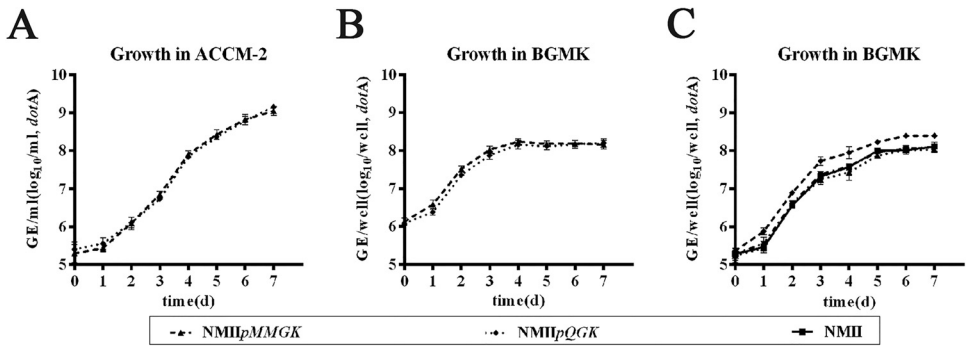

FIG 4 One-step growth curves of two transformants, NMII*pMMGK* and NMII*pQGK*, in axenic media (A) and BGMK cells (B, C). The one-step growth curves of *C. burnetii* inocula of two different origins, axenic media (A, B) and BGMK cells (C), were measured in axenic media (A) and BGMK cells (B, C). Regardless of the origin of *C. burnetii* inoculum, the two transformants showed similar growth kinetics. Bacterial growth was quantified by measuring genomic equivalents (GE).

QpH1-deficient *C. burnetii* almost completely fails to colonize murine bone marrow-derived macrophages. *In vitro*, *C. burnetii* can infect a variety of cell types, including epithelial and fibroblast cell lines. However, in natural infections, this bacterium has an infection tropism for mononuclear phagocytes (41). We next characterized the growth of NMII*pMMGK* and NMII*pQGK* transformants in human macrophage-like THP-1 cells and murine bone marrow-derived macrophages (murine BMDMs) (Fig. 6), both of which can support robust growth of *C. burnetii* phase II under normoxic culture conditions (42, 43). Equal multiplicity of infection (MOI) of two inocula (NMII*pMMGK* and NMII*pQGK*) from axenic media and three inocula (NMII*pMMGK*, NMII*pQGK*, and NMII) from BGMK cell cultures were used to infect the THP-1 and murine BMDM cells.

In THP-1 cells infected with inocula of the ACCM2 origin (Fig. 6A), NMII*pMMGK* has robust growth at 96 h postinfection, as shown by the densely packed bacterial clumps

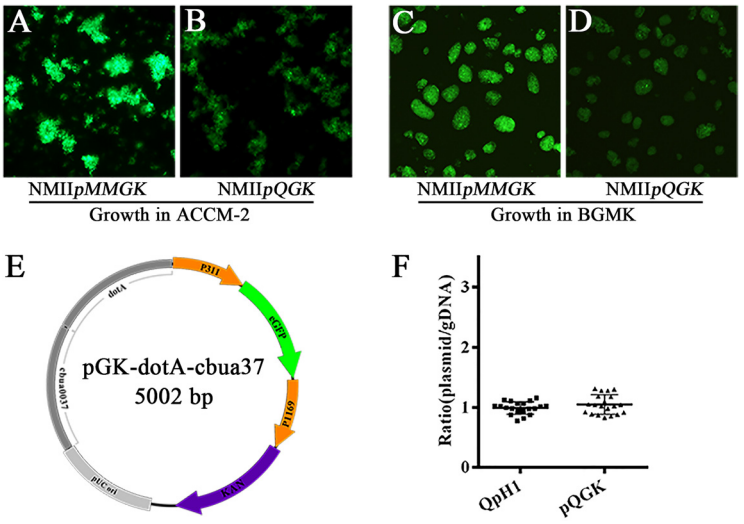

FIG 5 The RSF1010-ori-based vector pMMGK appears to have a greater copy number than the QpH1-based vector pQGK. (A to D) Fluorescence microscopy of NMII*pMMGK* (A, C) and NMII*pQGK* (B, D) in axenic media (A, B) and BGMK cells (C, D). It was clear that, in both axenic and BGMK cell cultures, NMII*pMMGK* consistently shows higher fluorescence intensity than NMII*pQGK*. The sequences of the eGFP gene and its promoters on both plasmids are identical. The higher level of eGFP expression in NMII*pMMGK* suggests a greater plasmid copy number of pMMGK. Paired images (A and B; C and D) were captured by using an inverted fluorescence microscope with the same image acquisition parameters. (E and F) A plasmid named pGK-dotA-cbua37 (E) was used as a standard for determining the plasmid copy numbers of QpH1 and pQGK by using qPCR (F). QpH1 and pQGK have similar copy numbers of approximately one, indicating that pQGK retains all of the genes required for plasmid replication and partitioning.

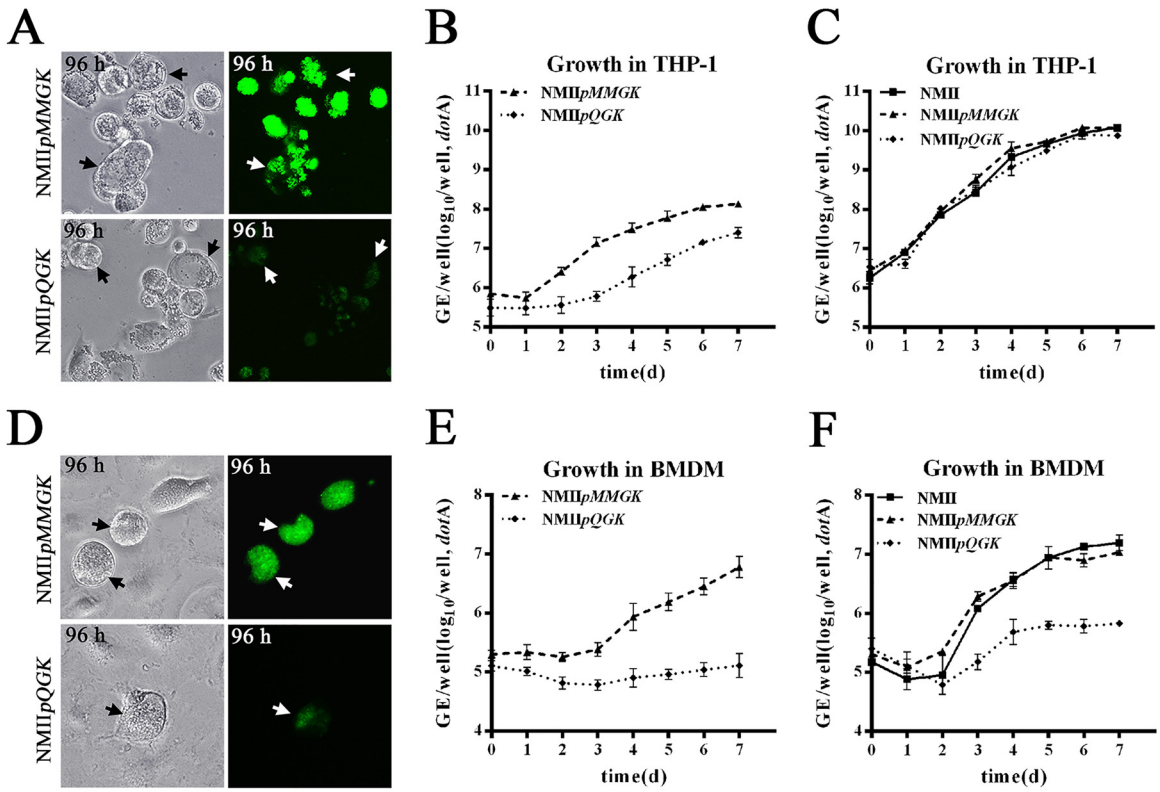

FIG 6 Growth of *C. burnetii* inocula prepared from axenic media (A, B, D, E) and BGMK cells (C, F) on macrophage-like THP-1 cells (A, B, C) and bone marrow-derived murine macrophages (BMDMs) (D, E, F). In THP-1 cells infected with *C. burnetii* of axenic culture origin (A, B), at 96 h postinfection, CCVs of NMII*pMMGK* have strong eGFP expression and are filled with bacterial particles while CCVs of NMII*pQGK* have weak eGFP expression and have fewer bacterial particles. Compared to NMII*pMMGK*, NMII*pQGK* has lower GEs at the initial attachment and lower growth yields throughout the culture period. In contrast, in THP-1 cells infected with *C. burnetii* of BGMK cell origin (C), *C. burnetii* Nine Mile II and its two transformants have nearly identical one-step growth curves and can be observed in THP-1 while infected with BGMK-cultured *C. burnetii*. In murine BMDMs infected with *C. burnetii* inocula prepared from axenic media (D, E), NMII*pMMGK* forms normal-size CCVs and has strong eGFP expression, while NMII*pQGK* almost completely fails to colonize. (D) A rarely observed CCV of NMII*pQGK* is shown. (E) The results of one-step growth curves are consistent with the above observations in murine BMDMs. After 7 days postinfection, NMII*pMMGK* has a growth yield of close to two logs while NMII*pQGK* has no significant growth. (F) To address the potential effects of axenic culture on *C. burnetii* viability, murine BMDM infections were repeated with *C. burnetii* inocula of BGMK cell origin. (F) In this case, compared to NMII*pMMGK*, NMII*pQGK* consistently showed a growth deficiency phenotype though minor growth yield of NMII*pQGK* was detected. In addition, the growth differences between varied NMII*pQGK* inocula in murine BMDMs are similar to the results of the above THP-1 cell infections. GEs of *C. burnetii* in THP-1 and BMDM cells represent four and three replicates, respectively.

and intensive eGFP expressions in its large CCVs. In contrast, NMII*pQGK* CCVs are partially filled with bacterial clumps and have lower eGFP expression. This evidently lower growth rate of NMII*pQGK* was confirmed by the one-step growth curves of these two strains (Fig. 6B). It is noted that the lower eGFP expression of NMII*pQGK* in THP-1 was likely due to a combination of lower plasmid copy number and lower growth rate. In addition, we repeatedly measured a lower ($P < 0.05$) number of NMII*pQGK* transformants at the infection time point of zero, which is the starting time after bacterial entry (Fig. 6B). Interestingly, the growth deficiency phenotypes of NMII*pQGK* were absent when infecting THP-1 cells with inocula from the BGMK cell cultures (Fig. 6C). In this case, NMII*pQGK* shared nearly identical growth profiles with NMII*pMMGK*. Therefore, the phenotypes in THP-1 cells with NMII*pQGK* of axenic origin reflect the effects that the axenic medium is likely to have on the bacterial colonization in human macrophages.

We next compared the growth of two transformants (NMII*pMMGK* and NMII*pQGK*) of different inoculum origins in murine BMDMs. First, the transformants of axenic origin were tested. In murine BMDMs at 96 h postinfection, NMII*pMMGK* forms normal CCVs that can be easily observed in any microscope field (Fig. 6D). This observation is consistent with the

previous finding of the robust growth of *C. burnetii* phase II in murine BMDMs (42). Contrarily, NMII*pQGK* produces almost zero CCVs. In our repeated experiments, only one NMII*pQGK* CCV was ever observed. This rarely observed CCV of NMII*pQGK* is shown in Fig. 6D. Consistent with microscopy observations, no growth of the NMII*pQGK* was detected by the quantitative PCR (qPCR) (Fig. 6E). In addition, comparison of the genome equivalent (GE) numbers at the starting time point of infection suggested that NMII*pQGK* also had slightly reduced attachment efficiency ($P < 0.05$), which was similar to findings in THP-1. Next, we characterized the growth of the transformants of cell culture origin in murine BMDMs (Fig. 6F). In this case, the NMII*pMMGK* growth yield was significantly improved compared to that of the aforementioned experiments using inocula of the axenic origin. Likewise, in comparison with the results of the experiments on using axenic medium-sourced inocula, the fluorescent CCVs of NMII*pQGK* could be more easily observed, and minor growth yield of NMII*pQGK* was also detected. The improved infection and growth yield of BGMK-sourced NMII*pQGK* inoculum were similar to results of the aforementioned experiments on the THP-1 infection. Despite the notable growth variations between alternative NMII*pQGK* inocula, the dramatic differences in both infection and growth between NMII*pMMGK* and NMII*pQGK* were consistently exhibited. Altogether, the murine BMDM infection results suggested that QpH1 is essential for *C. burnetii* survival in murine macrophages.

Plasmidless *C. burnetii* can be isolated by using CBUA0037- or CBUA0038-deleted shuttle vectors. The shuttle plasmid pQGK can be stably maintained and has a normal plasmid copy number in *C. burnetii* Nine Mile phase II. We next investigated the plasmid genes needed for the plasmid maintenance in pQGK. A PCR-based deletion mutagenesis approach was adopted to generate specific deletions in each of the five QpH1 ORFs (CBUA0036 to CBUA0039 and CBUA0039a) (Fig. 7A) (44). The deletion regions range from 60% to 100% of these ORFs. Primers with unique restriction enzyme sites at their 5′ ends were used for PCR amplification as described in Materials and Methods. After digestion with restriction enzymes, purified PCR products were ligated and transformed into *E. coli* Trans5α. The correctness of the desired plasmid construct was confirmed by sequencing. The plasmid knockout vectors are referred to as pQGK-D1, pQGK-D2, pQGK-D3, pQGK-D4, and pQGK-D5, corresponding to deletion mutants of CBUA0036, CBUA0037, CBUA0038, CBUA0039, and CBUA0039a, respectively.

Transformations of *C. burnetii* Nine Mile phase II with these knockout vectors were performed. All knockout vectors contained the eGFP cassette. Their transformants were cultured in kanamycin medium and were constantly observed using fluorescence microscopy. After passage five times, these transformants were cloned three times on semisolid plates. The cloned transformants were then cultured in kanamycin medium. The stability of the transformants was assessed via observing the eGFP expression. Transformation results are summarized in Table 1. Stable transformants carrying pQGK-D1 and pQGK-D5 were isolated (Fig. 7B). PCR detection of QpH1 genes indicated that QpH1 was also cured from these transformants. The results of pQGK-D1 and pQGK-D5 reveal that CBUA0036 and CBUA0039a are not required for stable plasmid maintenance in axenic culture of *C. burnetii*.

Transformation with other three deletion vectors yielded transient or unstable transformants in the presence of antibiotic selection. For the transformation with pQGK-D4, green fluorescence was observed at the first passage after electroporation but failed to expand in the presence of kanamycin selection. Importantly, the green fluorescence was repeatedly observed at the first passages in the repeated experiments. This transient eGFP expression suggested that pQGK-D4 was introduced into *C. burnetii* by electroporation but cannot be stably maintained.

Transformation with pQGK-D2 and pQGK-D3 produced significant bacterial yields in the presence of kanamycin selection. However, clones from kanamycin plates always gave a mixture of eGFP-positive and eGFP-negative bacterial clumps. Further identification of the eGFP-negative clones revealed that they were double deficient of QpH1 and the deletion mutant of pQGK (Fig. 7B and C). This unstable eGFP expression and the appearance of the plasmid-deficient *C. burnetii* suggested that pQGK-D2 and pQGK-D3 were incompatible with QpH1, and their transformants were constantly losing their shuttle plasmid due to the partitioning deficiency. A plasmid-deficient *C.*

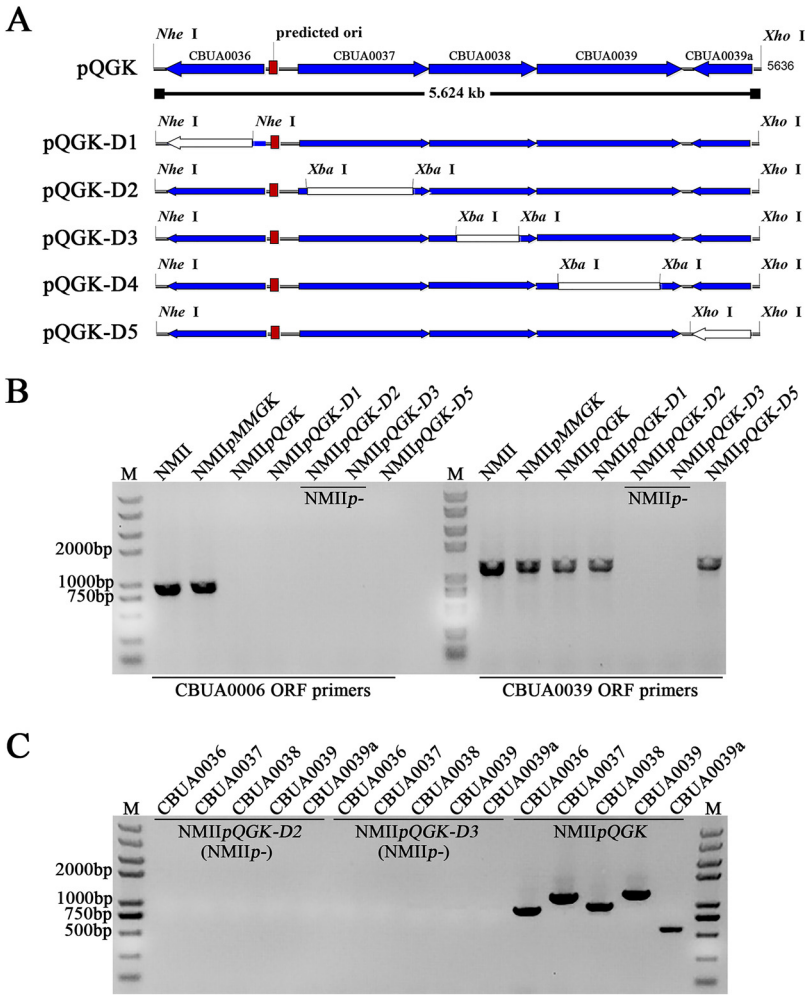

FIG 7 Construction of five individual QpH1 ORF knockout vectors and PCR identification of their transformants. (A) Schematic representation of deleted regions (white) of pQGK in five individual QpH1 ORF knockout vectors. The coding sequences of CBUA0036 to CBUA0039a and their direction of transcription are shown by the arrows on the line. (B) The CBUA0006 ORF is absent in transformants of pQGK, pQGK-D1, pQGK-D2, pQGK-D3, and pQGK-D5, suggesting that these transformants are QpH1 deficient. The CBUA0039 ORF is also absent in transformants of pQGK-D2 and pQGK-D3, suggesting that these two transformants contain no plasmid. (C) The CBUA0036 to CBUA0039a ORFs are absent in NMII*pQGK-D2* and NMII*pQGK-D3* but are present in NMII*pQGK*.

burnetii clone, NMIIp^-, was isolated by three successive clonings of pQGK-D2 transformants. Altogether, these results showed that CBUA0037, CBUA0038, and CBUA0039 are essential genes for QpH1 maintenance, and the pQGK-D2 and pQGK-D3 vectors are valuable tools for constructing plasmid-deficient *C. burnetii*.

TABLE 1 Viability and stability of *C. burnetii* Nine Mile phase II transformed with five pQGK deletion derivatives

	Phenotype of transformants growing in kanamycin medium	
Plasmid	**Bacterial growth[a]**	**eGFP stability**
pQGK-D1 (ΔCBUA0036)	+	Stable
pQGK-D2 (ΔCBUA0037)	+	Unstable
pQGK-D3 (ΔCBUA0038)	+	Unstable
pQGK-D4 (ΔCBUA0039)	−	Transient
pQGK-D5 (ΔCBUA0039a)	+	Stable

[a]Plus signs represent significant growth of kanamycin-resistant transformants, and minus signs represent the absence of noticeable growth of the transformants.

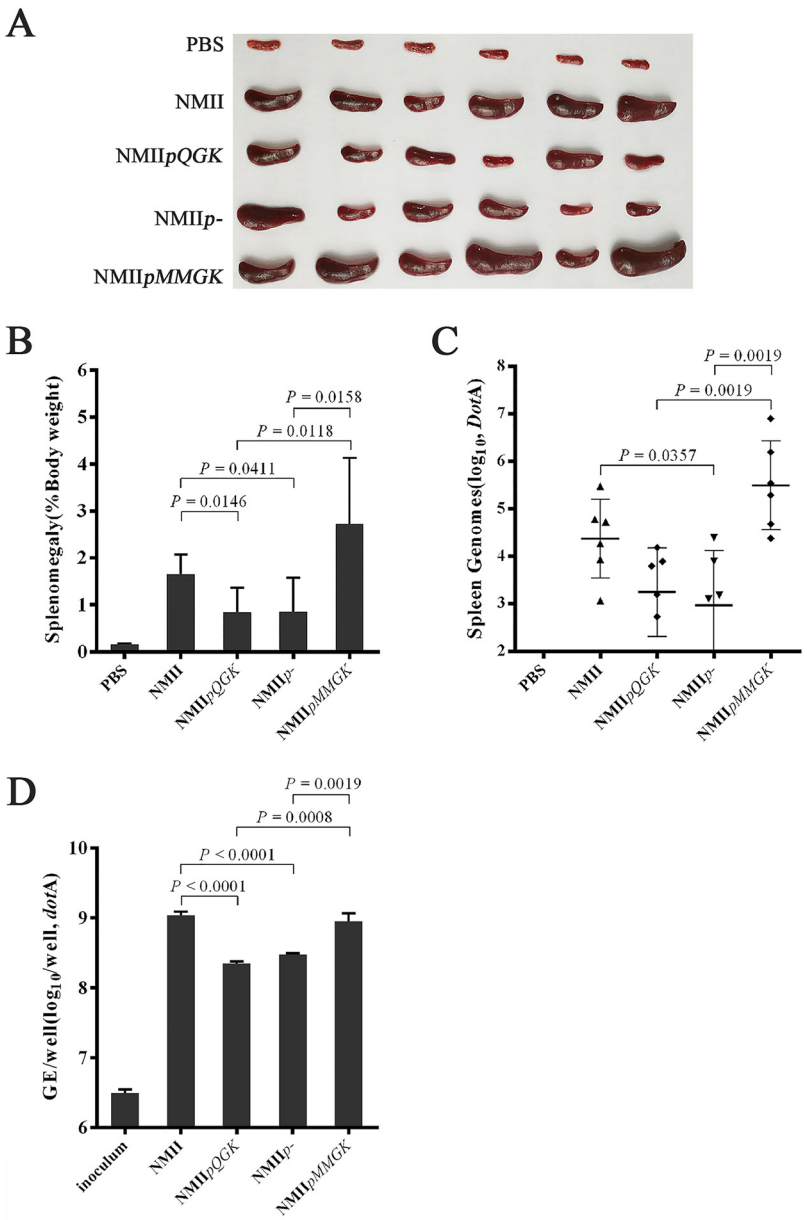

FIG 8 Splenomegaly of SCID mouse livers after intraperitoneal challenge with *C. burnetii*. SCID mice were challenged with PBS or 1×10^7 GE of *C. burnetii* via the intraperitoneal route and sacrificed 18 days after challenge. (A) Spleens were removed from control and challenged mice. (B) Splenomegaly calculated as spleen weight as a percentage of total body weight at the time of necropsy. QpH1-bearing strains (NMII and NMII*pMMGK*) caused bigger splenomegaly than QpH1-deficient strains (NMII*pQGK* and NMII*p*$^-$). (C) Genome equivalents calculated using TaqMan real-time PCR with DNA purified from infected spleens from 6 mice 18 days after challenge with *C. burnetii*. The *C. burnetii* genome equivalents are in accordance with the sizes of splenomegaly. (D) BMDMs generated from SCID mice were infected with *C. burnetii* strains—NMII, NMII*pMMGK*, NMII*pQGK*, and NMII*p*$^-$. All four strains have robust growth in SCID mouse originated BMDMs, though NMII*pQGK* and NMII*p*$^-$ appear to have lower growth yields than NMII and NMII*pMMGK*. For all panels, error bars represent standard deviations from the mean.

QpH1-deficient *C. burnetii* has reduced pathogenicity in SCID mice. The SCID mouse model was established for identifying virulence factors in *C. burnetii* phase II (45). We next analyzed the potential role of the plasmid in *C. burnetii* pathogenesis using this model (Fig. 8). Four *C. burnetii* strains—the parent Nine Mile phase II (NMII) and its three derivatives (NMII*pMMGK*, NMII*pQGK*, and NMII*p*$^-$)—were used to infect SCID mice by peritoneal injections. Compared to the phosphate-buffered saline (PBS)

control group, all four *C. burnetii* strains induced different levels of splenomegaly in infected mice (Fig. 8A and B). However, it is apparent that QpH1-bearing strains (NMII and NMII*pMMGK*) induced larger splenomegaly than QpH1-deficient strains (NMII*pQGK* and NMIIp^-) ($P < 0.05$), suggesting that QpH1 plays a role in pathogenicity. It is noted that NMII*pMMGK* had a tendency to cause bigger splenomegaly than its parent NMII ($P = 0.10$), indicative of the enhanced virulence by the pMMGK plasmid. This enhanced virulence of NMII*pMMGK* was likely associated with this strain's ability of normoxic growth. Characterization of *C. burnetii* normoxic growth has been described in a separate manuscript (46). Furthermore, the sizes of splenomegaly were in accordance with the *C. burnetii* genome equivalents in all infected mice (Fig. 8C). It is also obvious that NMII*pQGK* retained partial pathogenicity in SCID mice, which partially contradicts the aforementioned finding of NMII*pQGK* losing capability of colonizing murine BMDMs. Next, BMDMs from SCID mice were generated and infected with *C. burnetii* strains (Fig. 8D). Surprisingly, all four strains (NMII, NMII*pMMGK*, NMII*pQGK*, and NMIIp^-) had robust growth in SCID mouse-originated BMDMs, though NMII*pQGK* and NMIIp^- had lower growth yields than NMII and NMII*pMMGK*. These results could explain the partial pathogenicity of QpH1-deficient strains in SCID mice and suggested that the antimicrobial capacity of macrophages was dampened in this immunodeficiency mouse model. Altogether, our data suggested that QpH1 plays a partial role in the pathogenicity in the SCID mouse model.

DISCUSSION

All *C. burnetii* strains have one of the four different types of plasmids or one plasmid-like chromosomally integrated sequence. The plasmids' role in the *C. burnetii* biology has been implicated by the identification of type IV secretion effectors among its genes (4, 19). Our goal was to construct and characterize plasmid-deficient *C. burnetii*. We showed that QpH1-deficient *C. burnetii* Nine Mile phase II, NMII*pQGK*, can be constructed by transformation with a QpH1-based shuttle vector pQGK. The NMII*pQGK* strain had normal growth in axenic media and BGMK cells, displayed variable growth defects in human macrophages, and, most strikingly, showed severe infection deficiency in mouse BMDMs. In the SCID mouse model, the pathogenicity of the NMII*pQGK* strain was partially reduced. We showed that CBUA0037, CBUA0038, and CBUA0039 are essential ORFs for QpH1 maintenance, and unmarked QpH1-deficient mutants can be made by transformation with an unstable CBUA0037 or CBUA0038 deletion shuttle vector.

Plasmids are commonly classified by incompatibility (Inc) type (47), where the plasmids sharing the same replication mechanisms are incompatible. The Inc type of *C. burnetii* plasmids remains to be determined. An incompatible plasmid can be used for making plasmid-deficient *C. burnetii* strains. Our findings that pQGK can cure the endogenous QpH1 by transformation and had the same copy number of QpH1 indicated that pQGK retained an intact QpH1 replicon, including genes for plasmid replication, partitioning, and copy number control. The pQGK plasmid can be used for Inc typing of *C. burnetii* plasmids. The pQGK derivatives—pQGK-D2 or pQGK-D3—can be used for making unmarked plasmid-deficient mutants. *C. burnetii* has four types of plasmids. Therefore, this plasmid-curing approach has potential applications for investigation of the plasmid-type virulence of *C. burnetii*.

Plasmids can maintain their copy numbers by one of the three general classes of negative regulatory systems (48). Iterons (which are directly repeated DNA sequences playing an important role in regulation of plasmid copy number in bacterial cells) and their cognate replication (Rep) initiator proteins comprise the iteron-involved negative control system (49). Our results revealed that QpH1 is a low-copy-number plasmid and has atypical iterons. The replication and copy number control of QpH1 is likely regulated through the iteron-Rep complex. Iterons are able to exert plasmid incompatibility (50). Further studies are required to better understand the iterons involved in regulation of plasmid replication in *C. burnetii*. In addition, the role of the cognate RepA

protein (annotated as CBUA0039) was supported by our finding of the transient transformation with the pQGK-D4 vector. An AT-rich region, located between the iterons and CBUA0037, could be another essential element for QpH1 replication (51).

QpH1 is a plasmid with a low copy number (10). Low-copy-number plasmids have an active partitioning system. Two putative partitioning proteins, CBUA0036 (ParB) and CBUA0037 (ParA), have been annotated based on protein homology. Our results suggested that CBUA0037 and CBUA0038 are essential partitioning proteins, while CBUA0036 is nonessential for plasmid maintenance. The commonly used RSF1010-ori-based shuttle vectors for *C. burnetii* are also used in the genetic studies of *Legionella pneumophila* (33). Our identification of essential genes for QpH1 maintenance might be useful for future construction of QpH1-based shuttle vectors that can be stably maintained in *L. pneumophila*.

Besides genes for plasmid maintenance (replication, copy number control, and partitioning), plasmids from pathogenic microbes often contain genes associated with virulence and/or antibiotic resistance (44). Three of the 40 QpH1 ORFs are essential for plasmid maintenance. Most of the other ORFs likely contribute to *C. burnetii* virulence in various ways. Our finding of QpH1-deficient *C. burnetii* failing to colonize murine BMDMs likely explains the high conservation of plasmid genes in *C. burnetii*. We postulate that *C. burnetii* plasmids are essential for bacterial survival in natural reservoir hosts, including rodents. The role of rodents as a potential reservoir was suggested by finding *C. burnetii* infection in mice in different areas and countries (52–54).

How might plasmid genes contribute to the colonization of murine BMDMs? Previous studies using human cells found that the type IV secretion system and a repertoire of type IV effectors are required for the CCV biogenesis and *C. burnetii* growth (25–28). The roles of these type IV effectors in the *C. burnetii* pathogenicity are of intense interest (55). Plasmid-encoded effectors are possibly involved in the reduced growth efficiency of QpH1-deficient *C. burnetii* on THP-1 cells and might also be related to the failed colonization of murine BMDMs by QpH1-deficient *C. burnetii*. Newton and coworkers found that the effector proteins can be translocated as early as 1 h postinfection in murine BMDMs, while effector translocation can only be detected after 8 h postinfection in HeLa cells (56). We surmise that the early translocation of effectors might play an essential role in *C. burnetii* resistance to the antimicrobial activities of murine BMDMs. Further studies to investigate the pathogenesis of plasmid genes required for *C. burnetii* infection and growth in murine BMDMs are warranted.

The QpH1-deficient *C. burnetii* almost completely abrogates its capacity of infecting murine BMDMs. However, this mutant has only partially reduced pathogenicity in the SCID mice. Our subsequent finding of the capability of this mutant for robust growth in SCID mouse-sourced BMDMs was unexpected, as no impairment of macrophage functions had been reported in the SCID mouse. Relation of the DNA repair enzyme PRKDC of the SCID mouse to the macrophage's capability of restricting *C. burnetii* infection warrants further investigation as well. The immunocompetent animal model with *C. burnetii* phase I as control may be more appropriate for studying plasmid pathogenesis (12). It was also unexpected that the pMMGK transformant appeared to have enhanced pathogenicity. Though similar to other RSF1010-ori-based shuttle vectors, the pMMGK vector conferred an unexpected capability of normoxic growth on *C. burnetii*, which is likely to be related to the transformant's enhanced virulence. The normoxic growth of *C. burnetii* was characterized in a separate manuscript (46).

In conclusion, we investigated the functions of *C. burnetii* QpH1 plasmid genes. We propose that the intergenic region between CBUA0036 and CBUA0037 is the plasmid's origin of replication, and the plasmid's copy number is likely regulated through atypical iterons within this region. The CBUA0037, CBUA0038, and CBUA0039 ORFs encode two partitioning proteins and Rep proteins, respectively. QpH1 can be cured by transformation with pQGK or its two derivatives (pQGK-D2 and pQGK-D3). We present evidence that QpH1 is nonessential for *C. burnetii* growth in axenic media and BGMK cells. QpH1-deficient *C. burnetii* phase II has varied growth deficiency in human

macrophages depending on the origin of inocula. Most importantly, we found that QpH1 is essential for the *C. burnetii* colonization of murine BMDMs, suggesting an important role of this plasmid for the *C. burnetii* persistence in rodents. It is certain that more plasmid-related phenotypes remain to be identified. Our shuttle vectors will further the progress of genetic studies of *C. burnetii* and its plasmids. This work represents an important step toward unravelling the mystery of plasmid conservation in *C. burnetii*.

MATERIALS AND METHODS

Bacterial strains, cell lines, and key reagents. *C. burnetii* Nine Mile phase II (NMII) is from our laboratory strain collection and was passaged in ACCM-2 as previously described (22). *E. coli* Trans5α (TransGen Biotech) was used for recombinant DNA procedures and was grown in Luria-Bertani (LB) medium. Buffalo green monkey kidney (BGMK) cells were grown in RPMI 1640 medium (Gibco) supplemented with 10% fetal bovine serum (FBS) (Gibco). Human monocytic leukemia cells (THP-1) were cultured in high-glucose-containing Dulbecco's modified Eagle medium (DMEM) (Gibco) supplemented with 10% FBS. Murine bone marrow-derived macrophages (BMDM) were generated from C57BL/6JNifdc or SCID (CB17/Icr-*Prkdc*^{scid}/IcrIcoCrl) female mice as described by Cockrell et al. (42). Primers used in this study are listed in Tables S1 and S4 in the supplemental material. *Escherichia coli* Trans5α (TransGen Biotech) was used for all plasmid amplification.

Construction of an RSF1010-ori-based shuttle vector pMMGK. RSF1010-ori-based shuttle vectors are commonly used for *C. burnetii* transformation (30, 33). We constructed an RSF1010-ori-based vector pMMGK based on the backbone of pMMB207 (kindly provided by Xuehong Zhang from Shanghai Jiaotong University, Shanghai, China). Promoter regions of CBU0311 and CBU1169 were amplified with primer pairs P311-F/P311-R and P1169- F/P1169-R, respectively. The Kan^r and eGFP genes were amplified from pEASY-T1 and pEGFP-C1 with primer pairs Kan-F/Kan-R and eGFP-F/eGFP-R, respectively. Overlapping PCR with primers P311-F/Kan-R was used to produce the P311-eGFP-P1169-Kan^r segment. Two segments, pUC ori and ampicillin resistance gene (Amp^r), were amplified from pEASY-T1 with primer pairs pUC-F/pUC-R and Amp-F/Amp-R, respectively. Overlapping PCR with primers P311-F/pUC-R was used to produce the P311-eGFP-P1169-Kan^r-pUC ori segment. This segment and the Amp^r-containing segment were digested with NheI and XhoI and ligated to generate the vector pAGK. The RSF1010 backbone and the P311-eGFP-P1169-Kan^r segment were amplified from pMMB207 and pAGK, with primer pairs RSF1010-F/RSF1010-R and P311-F/KAN-R, respectively, and then were digested with NheI and XhoI and ligated to generate the shuttle vector pMMGK (see Appendix S2 in the supplemental material).

Construction of *C. burnetii* QpH1-based shuttle vector pQGK. The shuttle vector pQGK was constructed by replacing the Amp^r region of pAGK with a predicted region for plasmid replication and partitioning in QpH1. Briefly, a 5.6-kb segment covering CBUA0036 to CBUA0039a was amplified with primers pQ-F/pQ-R. PCR amplifications were performed in 100-μl reaction mixture volumes containing 50 ng DNA, a 0.2 mM concentration of each deoxynucleoside triphosphate (dNTP), a 0.2 μM concentration of each primer, 2.5 U TransStart FastPfu DNA polymerase (TransGen Biotech), and 20 μl buffer. PCR conditions were as follows: initial denaturation at 95°C for 4 min followed by 2 cycles of amplification at 95°C for 30 s, 55°C for 30 s, and 72°C for 1 min every 2 kb and then 28 cycles of amplification at 95°C for 30 s, 57°C for 30 s, and 72°C for 1 min every 2 kb and a final extension at 72°C for 10 min. This QpH1 segment and the pAGK plasmid were digested with NheI and XhoI and ligated to produce the shuttle plasmid pQGK (see Appendix S3 in the supplemental material).

Construction of deletion derivatives of pQGK. Deletion derivative of pQGK were constructed using a modified PCR-based approach (44). Primer pairs for knocking out CBUA0036 to CBUA0039a were shown in Table S1 in the supplemental material. Briefly, PCR amplifications were performed using TransStart FastPfu DNA polymerase (TransGen Biotech), and PCR conditions were described as above. PCR products were purified by a QIAquick PCR purification kit (Qiagen) and doubly digested with DMT (to remove template DNA) (TransGen Biotech) and restriction enzymes as indicated. Digested PCR products were ligated using Quick T4 DNA ligase (NEB) and transformed into *E. coli* Trans5α. Clones were screened for plasmids containing QpH1 ORFs but lacking the deleted region by PCR.

Transformation of *C. burnetii* Nine Mile phase II. All plasmids used in this study were purified using a plasmid maxi kit (Qiagen) and subjected to sequencing confirmation. The resulting vector was transformed into *C. burnetii* Nine Mile phase II by electroporation (31). For every passage after electroporation, *C. burnetii* was cultured at 2.5% O_2 and 5% CO_2 for 7 days in ACCM-2 containing 400 μg/ml kanamycin. Fluorescence microscopy was conducted to check eGFP expression after each passage. When eGFP expression was easily observed in bacterial clumps, semisolid agarose plates were then used for three successive clonings. *C. burnetii* and its transformants were expanded in ACCM-2. All *C. burnetii* and its transformants were suspended in SPG (0.25 M sucrose, 10 mM sodium phosphate, 5 mM L-glutamic acid) and kept frozen at −80°C.

PCR identification of transformants. The presence or absence of QpH1 in *C. burnetii* transformants was detected by PCR. Total DNAs were extracted using DNeasy blood and tissue kit (Qiagen) and then used as templates for PCR detection with TransTaq high-fidelity DNA polymerase (TransGen) and QpH1 gene primers (Table S4). PCR conditions are as follows: initial denaturation at 94°C for 5 min, followed by 35 cycles of 94°C for 30 s, 55°C for 30 s, 72°C for 90 s.

Plasmid relative copy number determination. The relative copy number of plasmids (QpH1 and pQGK) was determined by TaqMan qPCR. A plasmid standard derived from pAGK was first constructed. Briefly, an Amp^r-containing fragment of pAGK was replaced by a 0.85-kb *dotA* sequence fragment amplified from *C. burnetii* genomic DNA (gDNA) with primer pairs dotA-NheIF/dotA-XhoIR (containing NheI and XhoI) to form plasmid pGK-*dotA*. Then, a 0.83-kb cbua0037 sequence fragment amplified from QpH1 with primer pairs cbua37-XhoIF/cbua37-PciIR (containing XhoI and PciI) was inserted into plasmid pGK-*dotA* to produce pGK-dotA-cbua0037. Approximately 5×10^8 GEs for each *C. burnetii* and its transformant NMII*pQGK* were used, and total DNAs from NMII or NMII*pQGK* were extracted as above. Total DNAs were digested with EcoRV and purified by a QIAquick PCR purification kit (Qiagen). Two microliters of DNA for each was used as a template to determine the quantities of GE, QpH1, and pQGK through detection of *dotA* and CBUA0037 gene using primer pairs listed in Table S1, respectively. qPCR conditions were as follows: initial denaturation at 95°C for 10 min, followed by 40 cycles of amplification at 95°C for 15 s and 60°C for 1 min.

One-step growth curves. To measure the one-step growth curves in axenic media, seed stocks of *C. burnetii* were inoculated at a density of 2×10^6 GE/ml in 96-well plates containing 150 μl ACCM-2 medium per well. Cultures were incubated in a CO-170 tri-gas incubator at 37°C with 2.5% O_2 and 5% CO_2. Samples of axenic culture were collected at indicated time points and then were centrifuged at 20,000 $\times$ *g* for 10 min to harvest bacteria.

To measure the one-step growth curves in cells, bacterial inocula prepared from both ACCM-2 and BGMK cell cultures were used because, for unknown reasons, the infectivity of *C. burnetii* small-cell variants (SCVs) propagated in ACCM-2 is substantially less than that of host cell-propagated SCVs (23). Seed stocks of *C. burnetii* were plated onto 24-well cell (BGMK, THP-1, and BMDM) monolayers at the desired multiplicity of infection (MOI). Before experiment, confluent BGMK cells in T75 flasks were infected with *C. burnetii* at an MOI of 50, and infected cells were cultivated in 15 ml of RPMI supplemented with 2% FBS for 8 days. Then, after being washed with phosphate-buffered saline (PBS) (12.8 mM KH_2PO_4, 72.6 mM NaCl, 53.9 mM Na_2HPO_4, pH 7.4), infected cells were scraped in 10 ml PBS and disrupted by a 27-gauge needle connected to a syringe. Cell lysates were centrifuged at 2,500 $\times$ *g* for 10 min at 4°C. The supernatants were centrifuged at 20,000 $\times$ *g* for 30 min at 4°C, and pellets containing *C. burnetii* were resuspended with 1 ml of PBS, aliquoted, quantified, and frozen at −40°C. Before infection, BGMK cells (2.5×10^5 per well) were seeded in 24-well plates for 24-h cultivation, and confluent BGMK cells (approximate 5×10^5 per well) were infected with *C. burnetii* at an MOI of 20. THP-1 cells (2.5×10^5 per well) in 24-well plates were differentiated into macrophage-like cells by incubation overnight in DMEM containing 10% FBS and 200 nM phorbol myristate acetate (PMA) (Sigma-Aldrich) and were infected with *C. burnetii* at an MOI of 40. BMDM cells (2.0×10^5 per well) were infected with *C. burnetii* at an MOI of 40. The 24-well plates were centrifuged at 800 $\times$ *g* for 25 min at room temperature and placed in a CO_2 incubator (5% CO_2) at 37°C for 2 h. Cells were then washed twice with PBS and 1 ml cell medium was added to each well. At the indicated time, cell samples were harvested by using trypsin (HyClone) treatment and centrifugation.

Total DNAs were extracted with DNeasy blood and tissue kit (Qiagen). Genome copy numbers of *C. burnetii* in both axenic and cell cultures were determined by TaqMan probe qPCR as previously described (57).

Microscopy. *C. burnetii* cultures in ACCM-2 medium were incubated at 37°C for 7 days. Cells (BGMK, THP-1, and BMDM) grown in 24-well plates were infected with *C. burnetii* strains as described above and were incubated at 37°C for 96 h. Images were captured at a magnification of $\times$200 using an inverted fluorescence microscope (Zeiss Axio Observer D1) to record the bacterial clumps or CCV morphology of *C. burnetii* strains.

SCID mouse infections. SCID (CB17/Icr-*Prkdc*^{scid}/IcrIcoCrl) mice were purchased from Vital River Laboratory Animal Technology Co., Ltd (Beijing, China). Freshly ACCM-2-cultured *C. burnetii* and its transformants—NMII*p*$^-$, NMII*pMMGK*, and NMII*pQGK*—were diluted to 5×10^7 GE/ml in PBS. Six 6-week-old female mice per group were infected with 1×10^7 GE *C. burnetii* in 200 μl PBS via intraperitoneal injection. At 18 days postinfection, hearts, lungs, livers, and spleens were aseptically harvested and stored at −80°C; additionally, spleens were weighted to determine splenomegaly (spleen weight/body weight). All samples were individually added up to 2 ml with PBS and homogenized using a glass grinder. DNAs were purified from 20 μl tissue homogenate with DNeasy blood and tissue kit (Qiagen) and were used to determine *C. burnetii* GE by qPCR as described above. All animal experimental procedures involved were performed according to protocols approved by the Institutional Animal Care and Use Committee of Fifth Medical Center, General Hospital of Chinese PLA. The project ethics review approval number is IACUC-2018-0020.

Statistical analysis. A two-tailed Student's *t* test was used for comparison of splenomegaly and bacterial loads between different infection groups. The standard deviation was determined from three independent biological replicates.

SUPPLEMENTAL MATERIAL

Supplemental material is available online only.

SUPPLEMENTAL FILE 1, PDF file, 0.2 MB.

ACKNOWLEDGMENTS

This work was supported by Fundamental Research Funds for Central Universities (no. BUCTRC201917), NSFC International (regional) Cooperation and Exchange Program (no.

31961143024), Key Project of Beijing University of Chemical Technology (no. XK1803-06), National Natural Science Foundation of China (no. 31570177), and the State Key Program of National Natural Science of China (no. U1808202).

REFERENCES

1. Maurin M, Raoult D. 1999. Q fever. Clin Microbiol Rev 12:518–553. https://doi.org/10.1128/CMR.12.4.518.
2. Atlas RM. 2003. Bioterrorism and biodefence research: changing the focus of microbiology. Nat Rev Microbiol 1:70–74. https://doi.org/10.1038/nrmicro728.
3. Beare PA, Samuel JE, Howe D, Virtaneva K, Porcella SF, Heinzen RA. 2006. Genetic diversity of the Q fever agent, *Coxiella burnetii*, assessed by microarray-based whole-genome comparisons. J Bacteriol 188:2309–2324. https://doi.org/10.1128/JB.188.7.2309-2324.2006.
4. Voth DE, Beare PA, Howe D, Sharma UM, Samoilis G, Cockrell DC, Omsland A, Heinzen RA. 2011. The *Coxiella burnetii* cryptic plasmid is enriched in genes encoding type IV secretion system substrates. J Bacteriol 193:1493–1503. https://doi.org/10.1128/JB.01359-10.
5. Thiele D, Willems H, Haas M, Krauss H. 1994. Analysis of the entire nucleotide sequence of the cryptic plasmid QpH1 from *Coxiella burnetti*. Eur J Epidemiol 10:413–420. https://doi.org/10.1007/BF01719665.
6. Valkova D, Kazar J. 1995. A new plasmid (QpDV) common to *Coxiella burnetii* isolates associated with acute and chronic Q fever. FEMS Microbiol Lett 125:275–280. https://doi.org/10.1111/j.1574-6968.1995.tb07368.x.
7. Willems H, Ritter M, Jager C, Thiele D. 1997. Plasmid-homologous sequences in the chromosome of plasmidless *Coxiella burnetii* Scurry Q217. J Bacteriol 179:3293–3297. https://doi.org/10.1128/jb.179.10.3293-3297.1997.
8. Lautenschlager S, Willems H, Jager C, Baljer G. 2000. Sequencing and characterization of the cryptic plasmid QpRS from *Coxiella burnetii*. Plasmid 44:85–88. https://doi.org/10.1006/plas.2000.1470.
9. Jager C, Lautenschlager S, Willems H, Baljer G. 2002. *Coxiella burnetii* plasmid types QpDG and QpH1 are closely related and likely identical. Vet Microbiol 89:161–166. https://doi.org/10.1016/s0378-1135(02)00155-4.
10. Samuel JE, Frazier ME, Mallavia LP. 1985. Correlation of plasmid type and disease caused by *Coxiella burnetii*. Infect Immun 49:775–779. https://doi.org/10.1128/IAI.49.3.775-779.1985.
11. Thiele D, Willems H. 1994. Is plasmid based differentiation of *Coxiella burnetii* in 'acute' and 'chronic' isolates still valid? Eur J Epidemiol 10:427–434. https://doi.org/10.1007/BF01719667.
12. Long CM, Beare PA, Cockrell DC, Larson CL, Heinzen RA. 2019. Comparative virulence of diverse *Coxiella burnetii* strains. Virulence 10:133–150. https://doi.org/10.1080/21505594.2019.1575715.
13. Russell-Lodrigue KE, Andoh M, Poels MW, Shive HR, Weeks BR, Zhang GQ, Tersteeg C, Masegi T, Hotta A, Yamaguchi T, Fukushi H, Hirai K, McMurray DN, Samuel JE. 2009. *Coxiella burnetii* isolates cause genogroup-specific virulence in mouse and guinea pig models of acute Q fever. Infect Immun 77:5640–5650. https://doi.org/10.1128/IAI.00851-09.
14. Hornstra HM, Priestley RA, Georgia SM, Kachur S, Birdsell DN, Hilsabeck R, Gates LT, Samuel JE, Heinzen RA, Kersh GJ, Keim P, Massung RF, Pearson T. 2011. Rapid typing of *Coxiella burnetii*. PLoS One 6:e26201. https://doi.org/10.1371/journal.pone.0026201.
15. Hemsley CM, O'Neill PA, Essex-Lopresti A, Norville IH, Atkins TP, Titball RW. 2019. Extensive genome analysis of *Coxiella burnetii* reveals limited evolution within genomic groups. BMC Genomics 20:441. https://doi.org/10.1186/s12864-019-5833-8.
16. Stein A, Saunders NA, Taylor AG, Raoult D. 1993. Phylogenic homogeneity of *Coxiella burnetii* strains as determinated by 16S ribosomal RNA sequencing. FEMS Microbiol Lett 113:339–344. https://doi.org/10.1111/j.1574-6968.1993.tb06537.x.
17. Beare PA, Jeffrey BM, Martens CA, Heinzen RA. 2017. Draft genome sequences of the avirulent *Coxiella burnetii* Dugway 7D77-80 and Dugway 7E65-68 strains isolated from rodents in Dugway, Utah. Genome Announc 5:e00984-17. https://doi.org/10.1128/genomeA.00984-17.
18. Seshadri R, Paulsen IT, Eisen JA, Read TD, Nelson KE, Nelson WC, Ward NL, Tettelin H, Davidsen TM, Beanan MJ, Deboy RT, Daugherty SC, Brinkac LM, Madupu R, Dodson RJ, Khouri HM, Lee KH, Carty HA, Scanlan D, Heinzen RA, Thompson HA, Samuel JE, Fraser CM, Heidelberg JF. 2003. Complete genome sequence of the Q-fever pathogen *Coxiella burnetii*. Proc Natl Acad Sci U S A 100:5455–5460. https://doi.org/10.1073/pnas.0931379100.
19. Maturana P, Graham JG, Sharma UM, Voth DE. 2013. Refining the plasmid-encoded type IV secretion system substrate repertoire of *Coxiella burnetii*. J Bacteriol 195:3269–3276. https://doi.org/10.1128/JB.00180-13.
20. Guzman-Herrador DL, Steiner S, Alperi A, Gonzalez-Prieto C, Roy CR, Llosa M. 2017. DNA delivery and genomic integration into mammalian target cells through type IV A and B secretion systems of human pathogens. Front Microbiol 8:1503. https://doi.org/10.3389/fmicb.2017.01503.
21. Omsland A, Cockrell DC, Howe D, Fischer ER, Virtaneva K, Sturdevant DE, Porcella SF, Heinzen RA. 2009. Host cell-free growth of the Q fever bacterium *Coxiella burnetii*. Proc Natl Acad Sci U S A 106:4430–4434. https://doi.org/10.1073/pnas.0812074106.
22. Omsland A, Beare PA, Hill J, Cockrell DC, Howe D, Hansen B, Samuel JE, Heinzen RA. 2011. Isolation from animal tissue and genetic transformation of *Coxiella burnetii* are facilitated by an improved axenic growth medium. Appl Environ Microbiol 77:3720–3725. https://doi.org/10.1128/AEM.02826-10.
23. Sandoz KM, Beare PA, Cockrell DC, Heinzen RA. 2016. Complementation of arginine auxotrophy for genetic transformation of *Coxiella burnetii* by use of a defined axenic medium. Appl Environ Microbiol 82:3042–3051. https://doi.org/10.1128/AEM.00261-16.
24. Vallejo Esquerra E, Yang H, Sanchez SE, Omsland A. 2017. Physicochemical and nutritional requirements for axenic replication suggest physiological basis for *Coxiella burnetii* niche restriction. Front Cell Infect Microbiol 7:190. https://doi.org/10.3389/fcimb.2017.00190.
25. Beare PA, Gilk SD, Larson CL, Hill J, Stead CM, Omsland A, Cockrell DC, Howe D, Voth DE, Heinzen RA. 2011. Dot/Icm type IVB secretion system requirements for *Coxiella burnetii* growth in human macrophages. mBio 2:e00175-11. https://doi.org/10.1128/mBio.00175-11.
26. Carey KL, Newton HJ, Luhrmann A, Roy CR. 2011. The *Coxiella burnetii* Dot/Icm system delivers a unique repertoire of type IV effectors into host cells and is required for intracellular replication. PLoS Pathog 7:e1002056. https://doi.org/10.1371/journal.ppat.1002056.
27. Newton HJ, Kohler LJ, McDonough JA, Temoche-Diaz M, Crabill E, Hartland EL, Roy CR. 2014. A screen of *Coxiella burnetii* mutants reveals important roles for Dot/Icm effectors and host autophagy in vacuole biogenesis. PLoS Pathog 10:e1004286. https://doi.org/10.1371/journal.ppat.1004286.
28. Kohler LJ, Roy CR. 2015. Biogenesis of the lysosome-derived vacuole containing *Coxiella burnetii*. Microbes Infect 17:766–771. https://doi.org/10.1016/j.micinf.2015.08.006.
29. Martinez E, Cantet F, Fava L, Norville I, Bonazzi M. 2014. Identification of OmpA, a *Coxiella burnetii* protein involved in host cell invasion, by multiphenotypic high-content screening. PLoS Pathog 10:e1004013. https://doi.org/10.1371/journal.ppat.1004013.
30. Beare PA. 2012. Genetic manipulation of *Coxiella burnetii*. Adv Exp Med Biol 984:249–271. https://doi.org/10.1007/978-94-007-4315-1_13.
31. Beare PA, Heinzen RA. 2014. Gene inactivation in *Coxiella burnetii*. Methods Mol Biol 1197:329–345. https://doi.org/10.1007/978-1-4939-1261-2_19.
32. Beare PA, Sandoz KM, Omsland A, Rockey DD, Heinzen RA. 2011. Advances in genetic manipulation of obligate intracellular bacterial pathogens. Front Microbiol 2:97. https://doi.org/10.3389/fmicb.2011.00097.
33. Chen C, Banga S, Mertens K, Weber MM, Gorbaslieva I, Tan Y, Luo ZQ, Samuel JE. 2010. Large-scale identification and translocation of type IV secretion substrates by *Coxiella burnetii*. Proc Natl Acad Sci U S A 107:21755–21760. https://doi.org/10.1073/pnas.1010485107.
34. Lin Z, Howe D, Mallavia LP. 1995. Roa307, a protein encoded on *Coxiella burnetii* plasmid QpH1, shows homology to proteins encoded in the replication origin region of bacterial chromosomes. Mol Gen Genet 248:487–490. https://doi.org/10.1007/BF02191649.
35. Lin Z, Mallavia LP. 1994. Identification of a partition region carried by the plasmid QpH1 of *Coxiella burnetii*. Mol Microbiol 13:513–523. https://doi.org/10.1111/j.1365-2958.1994.tb00446.x.
36. Lin Z, Mallavia LP. 1995. The partition region of plasmid QpH1 is a member of a family of two trans-acting factors as implied by sequence analysis. Gene 160:69–74. https://doi.org/10.1016/0378-1119(95)00192-9.
37. Lin Z, Mallavia LP. 1998. Membrane association of active plasmid partitioning protein A in *Escherichia coli*. J Biol Chem 273:11302–11312. https://doi.org/10.1074/jbc.273.18.11302.

38. Lin Z, Mallavia LP. 1999. Functional analysis of the active partition region of the *Coxiella burnetii* plasmid QpH1. J Bacteriol 181:1947–1952. https://doi.org/10.1128/JB.181.6.1947-1952.1999.
39. Rice P, Longden I, Bleasby A. 2000. EMBOSS: the European Molecular Biology Open Software Suite. Trends Genet 16:276–277. https://doi.org/10.1016/s0168-9525(00)02024-2.
40. Sarachu M, Colet M. 2005. wEMBOSS: a web interface for EMBOSS. Bioinformatics 21:540–541. https://doi.org/10.1093/bioinformatics/bti031.
41. Voth DE, Heinzen RA. 2007. Lounging in a lysosome: the intracellular lifestyle of *Coxiella burnetii*. Cell Microbiol 9:829–840. https://doi.org/10.1111/j.1462-5822.2007.00901.x.
42. Cockrell DC, Long CM, Robertson SJ, Shannon JG, Miller HE, Myers L, Larson CL, Starr T, Beare PA, Heinzen RA. 2017. Robust growth of avirulent phase II *Coxiella burnetii* in bone marrow-derived murine macrophages. PLoS One 12:e0173528. https://doi.org/10.1371/journal.pone.0173528.
43. Hayek I, Fischer F, Schulze-Luehrmann J, Dettmer K, Sobotta K, Schatz V, Kohl L, Boden K, Lang R, Oefner PJ, Wirtz S, Jantsch J, Luhrmann A. 2019. Limitation of TCA cycle intermediates represents an oxygen-independent nutritional antibacterial effector mechanism of macrophages. Cell Rep 26:3502–3510. https://doi.org/10.1016/j.celrep.2019.02.103.
44. Song L, Carlson JH, Whitmire WM, Kari L, Virtaneva K, Sturdevant DE, Watkins H, Zhou B, Sturdevant GL, Porcella SF, McClarty G, Caldwell HD. 2013. *Chlamydia trachomatis* plasmid-encoded Pgp4 is a transcriptional regulator of virulence-associated genes. Infect Immun 81:636–644. https://doi.org/10.1128/IAI.01305-12.
45. van Schaik EJ, Case ED, Martinez E, Bonazzi M, Samuel JE. 2017. The SCID mouse model for identifying virulence determinants in *Coxiella burnetii*. Front Cell Infect Microbiol 7:25. https://doi.org/10.3389/fcimb.2017.00025.
46. Luo S, He Z, Sun Z, Yu Y, Jiang Y, Tong Y, Song L. 2019. Culture under normoxic conditions and enhanced virulence of phase II Coxiella burnetii transformed with a RSF1010-based shuttle vector. bioRxiv https://doi.org/10.1101/747220.
47. Couturier M, Bex F, Bergquist PL, Maas WK. 1988. Identification and classification of bacterial plasmids. Microbiol Rev 52:375–395. https://doi.org/10.1128/MR.52.3.375-395.1988.
48. del Solar G, Espinosa M. 2000. Plasmid copy number control: an ever-growing story. Mol Microbiol 37:492–500. https://doi.org/10.1046/j.1365-2958.2000.02005.x.
49. Chattoraj DK. 2000. Control of plasmid DNA replication by iterons: no longer paradoxical. Mol Microbiol 37:467–476. https://doi.org/10.1046/j.1365-2958.2000.01986.x.
50. Rawlings DE, Tietze E. 2001. Comparative biology of IncQ and IncQ-like plasmids. Microbiol Mol Biol Rev 65:481–496. https://doi.org/10.1128/MMBR.65.4.481-496.2001.
51. Rajewska M, Wegrzyn K, Konieczny I. 2012. AT-rich region and repeated sequences—the essential elements of replication origins of bacterial replicons. FEMS Microbiol Rev 36:408–434. https://doi.org/10.1111/j.1574-6976.2011.00300.x.
52. El-Mahallawy HS, Lu G, Kelly P, Xu D, Li Y, Fan W, Wang C. 2015. Q fever in China: a systematic review, 1989–2013. Epidemiol Infect 143:673–681. https://doi.org/10.1017/S0950268814002593.
53. Stoenner HG, Lackman DB. 1960. The biologic properties of *Coxiella burnetii* isolated from rodents collected in Utah. Am J Hyg 71:45–51. https://doi.org/10.1093/oxfordjournals.aje.a120088.
54. Liu L, Baoliang X, Yingqun F, Ming L, Yu Y, Yong H, Shasha W, Manxia H, Tianyu G, Chao J, Xiaohong S, Jing W. 2013. *Coxiella burnetii* in rodents on Heixiazi Island at the Sino-Russian border. Am J Trop Med Hyg 88:770–773. https://doi.org/10.4269/ajtmh.12-0580.
55. Cunha LD, Ribeiro JM, Fernandes TD, Massis LM, Khoo CA, Moffatt JH, Newton HJ, Roy CR, Zamboni DS. 2015. Inhibition of inflammasome activation by *Coxiella burnetii* type IV secretion system effector IcaA. Nat Commun 6:10205. https://doi.org/10.1038/ncomms10205.
56. Newton HJ, McDonough JA, Roy CR. 2013. Effector protein translocation by the *Coxiella burnetii* Dot/Icm type IV secretion system requires endocytic maturation of the pathogen-occupied vacuole. PLoS One 8:e54566. https://doi.org/10.1371/journal.pone.0054566.
57. Wang T, Yu Y, Liang X, Luo S, He Z, Sun Z, Jiang Y, Omsland A, Zhou P, Song L. 2018. Lipid A has significance for optimal growth of *Coxiella burnetii* in macrophage-like THP-1 cells and to a lesser extent in axenic media and non-phagocytic cells. Front Cell Infect Microbiol 8:192. https://doi.org/10.3389/fcimb.2018.00192.